

Heat-capacity and magnetic measurements on the $Y(Ni_{2-x}Co_x)B_2C$ system

C. C. Hoellwarth, P. Klavins, and R. N. Shelton

Department of Physics, University of California, Davis, California 95616

(Received 21 September 1995)

We have performed field- and temperature-dependent magnetization, resistivity, and heat-capacity measurements on polycrystalline samples of the $Y(Ni_{2-x}Co_x)B_2C$ system with $0.0 \leq x \leq 0.4$. Values of T_c , χ_0 , H_{c2} , Θ_D , λ , and $N(E_f)$ were determined for various samples. We observe that Θ_D increases with x , while all the other parameters decrease with x . The T_c vs x data can be described using the BCS theory and the measured values of $N(E_f)$ and Θ_D . The results suggest that the decrease in T_c is due to the decrease in $N(E_f)$, in agreement with the results from band structure calculations.

INTRODUCTION

The discovery of superconductivity in the RNi_2B_2C ($R = Sc, Y, Lu, Er, Tm, Ho$) system^{1,2} has generated widespread interest among experimentalist and theorists alike. This system forms a filled variant of the $ThCr_2Sr_2$ structure having alternating YC and Ni_2B_2 layers,³ similar to the high- T_c oxides. Unlike the high- T_c oxides, these materials appear to be traditional electron-phonon coupled superconductors. It is believed that superconductivity exists in this system due to a large density of electronic states at the Fermi level and a moderately strong electron-phonon interaction.⁴ There is a systematic decrease in T_c with increasing magnetic moment of the rare earth ions, scaling roughly with the deGennes factor.⁵ This behavior indicates that T_c decreases due to weak magnetic interactions between the rare earth ions and the conduction electrons. Mattheiss *et al.*⁶ put forth the idea that the superconductivity is highly correlated with the Ni-B-Ni bond angle. Changing the angle, by increasing the size of the rare earth ion, changes the density of states at the Fermi level, accounting for the decrease in T_c and the eventual disappearance of superconductivity.

Band structure calculations predict a peak in the density of states at the Fermi level for YNi_2B_2C and $LuNi_2B_2C$, with a large contribution coming from the $3d$ nickel bands.⁷⁻⁹ Similar calculations on $LuCo_2B_2C$ predict that the density of states at the Fermi level lies in a valley, explaining the lack of superconductivity in this compound. Assuming a rigid band model and BCS superconductivity, even small amounts of Co doped into the Ni site could lead to large reductions in T_c due to a shift in the value of the density of states. Previous doping studies on polycrystalline samples indicate that Co alloying destroys superconductivity with 20% substitution of Co for Ni.¹⁰⁻¹² Possible explanations for this change are a reduction in the density of states at the Fermi level and/or a change in the electron-phonon coupling strength. To study these effects further we present low temperature heat capacity measurements on samples in the system $Y(Ni_{2-x}Co_x)B_2C$ with $x=0.02, 0.2, 0.4$ and magnetization and electron transport measurements on samples with $x=0.00, 0.05, 0.10, 0.15, 0.20, 0.25, 0.35$.

EXPERIMENTAL DETAILS

Samples were made by melting high purity Y (Ames Lab), Ni (99.998%), Co (99.9975%), B (99.999%), C (99.9%) on a

standard water cooled copper hearth in a zirconium gettered argon atmosphere. The button was turned over and remelted three times to ensure sample homogeneity. Mass losses for the samples ranged between 0.3% and 1%. The samples were wrapped in tantalum foil, vacuum sealed in quartz tubes and annealed at 1050 °C. Samples used for magnetization and electrical resistivity studies were approximately 0.2 g and annealed for 2 days. Samples used for heat capacity were approximately 5 g and were annealed for 9 days.

All samples were characterized by powder x-ray diffraction using $Cu K\alpha$ radiation in a Siemens D500 diffractometer. Lattice parameters were determined using a standard least squares fit. The majority of samples were single phase. Magnetization samples with $x=0.05, 0.15, 0.25$ had impurities that could be identified as YiN_4B and $YNiBC$ with impurity levels under 3%; heat capacity samples with $x=0.02$ and 0.04 had impurities that could be identified as YB_2C_2 with impurity levels under 3% as well.

Magnetization and resistivity studies were performed on rectangular samples with dimensions approximately $1 \times 1 \times 3$ mm. Resistivity measurements were done using a standard four-probe technique. Magnetization measurements were done in a commercial superconducting quantum interference device (SQUID) magnetometer.¹³

Heat capacity data were taken in fields of 0 and 7 T using

TABLE I. Superconducting transition temperature, upper critical field, and lattice parameters for compounds in the system $Y(Ni_{2-x}Co_x)B_2C$. (*) Determined from heat capacity. (**) Measurement was not performed.

x	T_c (K)	ΔT_c (K)	$H_{c2}(0)$	a (nm)	c (nm)
0.00	14.5	1.0	5.9	0.352 60	1.0533
0.025	13.0	2.0	4.3	0.352 56	1.0529
0.05	11.0	2.0	3.2	0.352 56	1.0530
0.10	9.5	1.2	2.3	0.352 55	1.0530
0.15	7.5	2.0	1.6	0.352 55	1.0524
0.20	5.7	2.0	1.2	0.352 52	1.0522
0.25	4.5	5.0	**	0.352 45	1.0515
0.30	2.7	1.5	**	0.352 45	1.0515
0.35	2.0	2	**	0.352 44	1.0514
0.40	1.6*	1*	**	0.352.34	1.0502

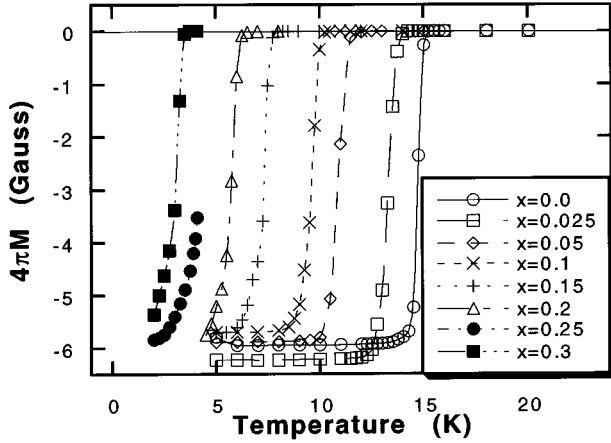


FIG. 1. Superconducting transitions for samples of the $Y(Ni_{2-x}Co_x)B_2C$ system in a field of 5 Oe.

a semiadiabatic heat pulse technique. The heat capacity data are accurate to within 2% in zero field and 4% at 7 T.

RESULTS AND DISCUSSION

The structural space group for the entire $Y(Ni_{2-x}Co_x)B_2C$ series is $I4/mmm$. The lattice parameters decrease slightly with increasing Co concentration, the decrease for both a and c is less than 0.5% over the superconducting region. The values for a and c are listed in Table I. These values are consistent with the results of Braun¹⁰ and Gangopadhyay.¹¹

The transition temperature T_c was taken to be the midpoint of the superconducting transition (Fig. 1) in a field of 5 Oe. All of the samples have transition widths less than 2 K, except for $x=0.25$ which has $\Delta T_c=5$ K, with superconducting volume fractions that are consistent with 100% shielding. The onset temperature for the $x=0.0$ sample was 15.2 K consistent with values reported in the literature.^{1,10,11,14,15} A plot of T_c versus x is shown in Fig. 2. The measurements of the superconducting transition temperatures from heat capacity and magnetization agree very well. The transition temperature is a strong nonlinear function of Co concentration, with T_c going from 14.5 K at $x=0.0$ to 1.6 K; at $x=0.4$.

The upper critical field H_{c2} is determined from resistance

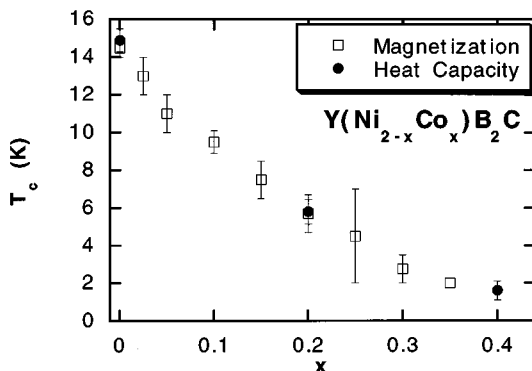


FIG. 2. The superconducting transition temperature, T_c , versus cobalt concentration x .

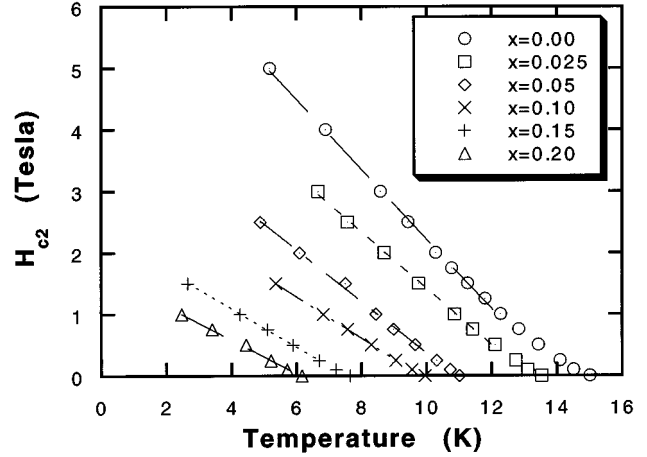


FIG. 3. Upper critical field, H_{c2} , versus temperature for samples of the $Y(Ni_{2-x}Co_x)B_2C$ system for different Co concentrations. The curves are fits to the linear region of the data.

vs temperature measurements at various fields. The critical temperature at a specified field is given by the midpoint of the superconducting transition. Figure 3 plots the critical temperature versus the specific field H_{c2} for $0.0 \leq x \leq 0.2$. A value for $H_{c2}(0)$ can be estimated using the Werthamer, Helfand, and Hohenberg (WWH) equation:¹⁶

$$H_{c2}(0) = -0.69T_c \left. \frac{dH_{c2}(T)}{dT} \right|_{T=T_c}. \quad (1)$$

Values for $H_{c2}(0)$ are listed in Table I. The results show that the upper critical field decreases nonlinearly with x .

The heat capacity results for both 0 and 7 T are plotted in Figs. 4(a) and 4(b), and 4(c) for $x=0.0, 0.2, 0.4$. The superconducting state was completely suppressed using a 7 T field for the samples with $x=0.0$ and 0.2. The $x=0.4$ sample is normal to below 2 K so it was not deemed necessary to measure the sample in a field. The normal state data below 10 K were fit to the form:

$$C_p = \gamma T + \beta T^3, \quad (2)$$

where γT is the electronic heat capacity and βT^3 is the lattice heat capacity. An estimate of the Debye temperature can be determined from values of β using the following equation:

$$\Theta_D = \left[\frac{12\pi^4 N r k_b}{5\beta} \right]^{1/3}, \quad (3)$$

where k_b is the Boltzmann constant, r is the number of atoms per molecule, and N is the number of molecules. As the Co concentration is varied, Θ_D increases slightly with increasing x . The quantitative values derived from these fits of the data are listed in Table II.

The γ term is related to the density of states at the Fermi level by the following relation:

$$\gamma = \frac{1}{3} \pi^2 k_b^2 N^*(E_f), \quad (4)$$

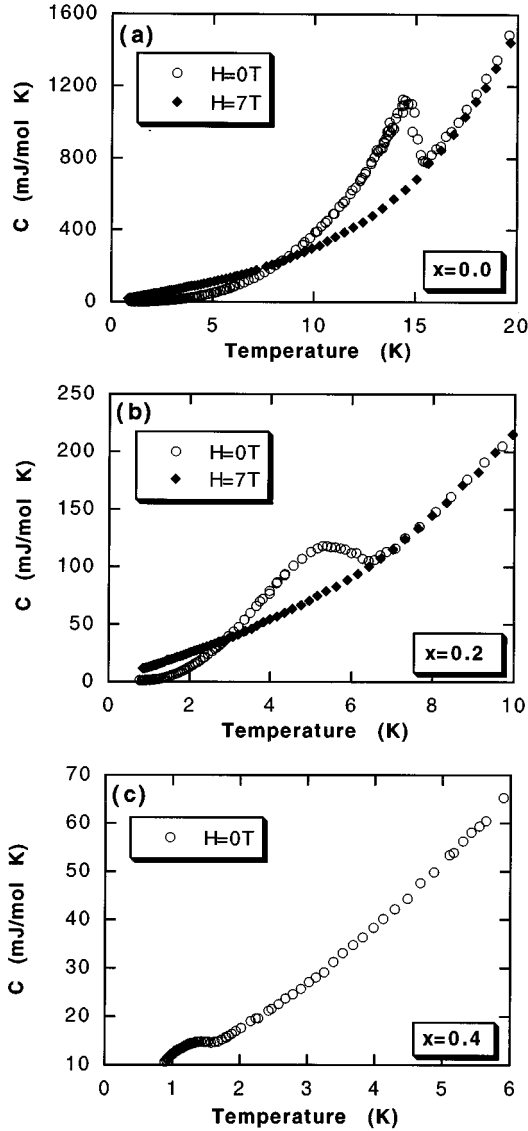


FIG. 4. (a) Heat capacity versus temperature for $\text{YNi}_2\text{B}_2\text{C}$ over the temperature range 0.7 to 20 K in fields of 0 and 7 T. (b) Heat capacity versus temperature for $\text{YNi}_{1.8}\text{Co}_{0.2}\text{B}_2\text{C}$ over the temperature range 0.7 to 10 K in fields of 0 and 7 T. (c) Heat capacity versus temperature for $\text{YNi}_{1.6}\text{Co}_{0.4}\text{B}_2\text{C}$ over the temperature range 0.7 to 6 K.

where $N^*(E_f)$ is the enhanced density of states. The density of states is enhanced due to electron-phonon interactions, which effectively increase the mass of the electron. This in turn increases $N(E_f)$ so that

$$N^*(E_f) = \frac{m^*}{m} N_b(E_f) = (1 + \lambda) N_b(E_f), \quad (5)$$

where $N_b(E_f)$ is the density of states in the absence of electron-phonon interactions or the bare density of states, m^* is the effective mass of the electron, and λ is the electron-phonon coupling constant. There is a strong nonlinear decrease in both γ and $N^*(E_f)$ as x increases. The results are listed in Table II.

TABLE II. Parameters derived from heat capacity and magnetic susceptibility data for compounds in the system $\text{Y}(\text{Ni}_{2-x}\text{Co}_x)\text{B}_2\text{C}$.

x	γ (mJ/mol K ²)	Θ_D (K)	$N^*(E_f)$ (states/eV atom spin)	χ_0 (1/g $\times 10^{-7}$)	$N_b(E_f)$ (states/eV atom spin)	λ
0.0	19.8	480	0.701	8.3	0.334	1.10
0.2	12.0	490	0.423	5.7	0.250	0.69
0.4	8.03	500	0.283	4.1	0.212	0.34

Estimates for λ and $N_b(E_f)$ were obtained using Eq. (5) and measurements of the temperature independent dc magnetic susceptibility, χ_0 . A value for χ_0 was obtained by fitting the susceptibility vs temperature data to the equation

$$\chi = \chi_0 + \frac{C}{(T - T_a)}, \quad (6)$$

where χ_0 is the temperature independent susceptibility and $C/(T - T_a)$ is assumed to be due to the weak paramagnetism of magnetic impurities. Values for χ_0 obtained from fitting the data are listed in Table II. The temperature independent dc magnetic susceptibility is the sum of the core diamagnetism, Landau diamagnetism, and the Pauli paramagnetism:

$$\chi_0 = \chi_{\text{core}} + \chi_{\text{Landau}} + \chi_{\text{Pauli}}. \quad (7)$$

The value for χ_{core} was determined from standard tables¹⁷ and is estimated to be 3.6×10^{-5} emu/mole; χ_{Landau} and χ_{Pauli} are given by the following equations:

$$\chi_{\text{Landau}} = \frac{-1}{3(1 + \lambda)^2} \chi_{\text{Pauli}} \quad \text{and} \quad \chi_{\text{Pauli}} = 2\mu_b^2 N_b(E_f).$$

Thus

$$\chi_0 - \chi_{\text{core}} = 2\mu_b^2 \left(1 - \frac{1}{3(1 + \lambda)^2} \right) N_b(E_f). \quad (8)$$

Because $\chi_0 - \chi_{\text{core}}$ and $N^*(E_f)$ are determined experimentally, λ and $N_b(E_f)$ can be determined experimentally, λ and $N_b(E_f)$ can be calculated by solving Eq. (5) and Eq. (8) simultaneously. The results are listed in Table II. The values for $N_b(E_f)$ are quite large, ranging between 0.334 and 0.212 (states/ev atom spin); values for λ range between 1.10 and 0.34. These results are consistent with the superconductivity being due to a moderate electron phonon coupling and a large $N(E_f)$. The values for $N(E_f)$ and λ decrease sharply with Co substitution indicating that there is a peak in the density of states in agreement with band structure calculations.^{6,8,9}

There is evidence that the borocarbides are conventional BCS superconductors. For a BCS superconductor, the transition temperature is proportional to the quantity $T_c \approx \Theta_D \exp[-1/N(E_f)V]$ where V is a parameter describing the electron-phonon coupling strength. In this expression, the transition temperature is very sensitive to changes in $N(E_f)$ or V and only moderately sensitive to changes in Θ_D . Based on our results, the variation of Θ_D as Co is substituted for Ni can be expressed by the equation $\Theta_D = 480 + 50x$. Similarly,

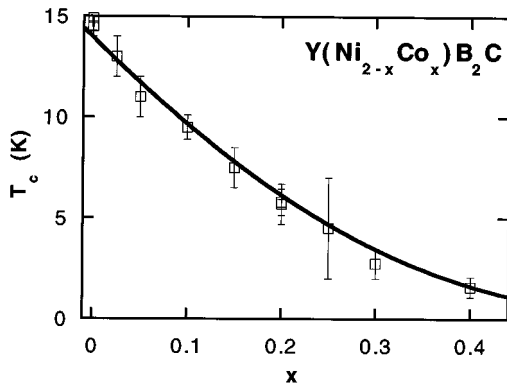


FIG. 5. Superconducting critical temperature versus concentration. The curve is Eq. (5); see text for details.

$N(E_f)$ can be expressed by the equation $N(E_f) = 0.326 - 0.305x$. Substituting these values into the BCS equation yields

$$T_c = 1.13(480 + 50x) \exp\left[\frac{-1}{(0.326 - 0.305x)V}\right]. \quad (9)$$

Equation (9) with $V = 0.838$ is in excellent agreement to the T_c vs x data, as shown in Fig. 5. Only $N(E_f)$ and Θ_D vary with Co concentration. Since Θ_D is increasing with x , the disappearance of superconductivity with Co doping can be explained by the decrease in the density of states at the Fermi level. Band structure calculations predict a peak in the $N(E_f)$ with large contributions from the Ni $3d$ electrons.

Assuming a rigid band model, cobalt, which has one less $3d$ electron than nickel, will decrease the position of the Fermi energy, moving $N(E_f)$ away from the peak. A rigid band model appears to be valid because the lattice parameters are essentially unchanged as Co is doped into the material and because Co and Ni are neighbors having similar electronic structure and atomic size. Thus the borocarbides appear to be conventional superconductors. Experimentally, T_c and $N(E_f)$ do decrease with Co doping. Furthermore, the decreasing $N(E_f)$ lowers the T_c as described by the BCS equation.

CONCLUSION

In summary, we have performed measurements of T_c , H_{c2} , χ_0 , Θ_D , and γ from which we determined $N(E_f)$ and λ . The results show that there is a peak in $N(E_f)$ verifying predictions from band structure calculations. This implies that the electronic contributions, especially the $3d$ nickel electrons, are very important to the superconductivity in these materials. The decrease in T_c with x can be explained by the cobalt concentration dependence of Θ_D , $N(E_f)$, and the BCS theory. This is further confirmation that the superconductivity in the borocarbides is conventional BCS in nature. The large $N(E_f)$ and the moderate electron phonon coupling strength lead to the rather high transition temperatures.

ACKNOWLEDGMENTS

This work was supported by National Science Foundation, Grant No. DMR94-03895.

¹R. J. Cava *et al.*, Nature **372**, 245 (1994).

²H. C. Ku, C. C. Lai, Y. B. You, J. H. Shieh, and W. Y. Guan, Phys. Rev. B **50** (1994).

³T. Siegrist, H. W. Zandbergen, R. J. Cava, J. J. Krajewski, and W. F. Peck, Nature **367**, 254 (1994).

⁴S. A. Carter, B. Batlogg, R. J. Cava, J. J. Krajewski, and W. F. Peck, Phys. Rev. B **50**, 4216 (1994).

⁵H. Eisaki *et al.*, Phys. Rev. B **50**, 647 (1994).

⁶L. F. Mattheiss, T. Siegrist, and R. J. Cava, Solid State Commun. **91**, 587 (1994).

⁷L. F. Mattheiss, Phys. Rev. B **49**, 13 279 (1994).

⁸W. E. Pickett and D. J. Singh, Phys. Rev. Lett. **72**, 3702 (1994).

⁹R. Coehoorn, Physica C **228**, 331 (1994).

¹⁰H. Schmidt, M. Müller, and H. F. Braun, Physica C **235-240**, 779 (1994).

¹¹A. K. Gangopadhyay, A. J. Schuetz, and J. S. Schilling, Physica C **246**, 317 (1995).

¹²S. J. Bud'ko *et al.*, Physica C **243**, 183 (1995).

¹³Quantum Design, 11578 Sorrento Valley Road, San Diego, CA 92121.

¹⁴S. B. Roy *et al.*, Physica C **228**, 319 (1994).

¹⁵R. Prozorov, E. R. Yacoby, I. Felner, and Y. Yoshurun, Physica C **233**, 367 (1994).

¹⁶N. R. Werthamer, E. Helfand, and P. C. Hohenberg, Phys. Rev. **147**, 295 (1966).

¹⁷P. W. Selwood, *Magnetochemistry* (Interscience Publishers, New York, 1956), p. 78.